

Nitrogen and oxygen availabilities control water column nitrous oxide production during seasonal anoxia in the Chesapeake Bay

Qixing Ji¹, Claudia Frey¹, Xin Sun¹, Melanie Jackson², Yea-Shine Lee¹, Amal Jayakumar¹, Jeffrey C. Cornwell² and Bess B. Ward¹

¹Department of Geosciences, Princeton University, Princeton, 08544, New Jersey, USA

²Horn Point Laboratory, University of Maryland Center for Environmental Science, Cambridge, 21613, Maryland, USA

Correspondence to: Qixing Ji (qji@princeton.edu)

Abstract. Nitrous oxide (N₂O) is a greenhouse gas and an ozone depletion agent. Estuaries are generally regarded as N₂O sources. However, insufficient understanding of the environmental controls on N₂O production results in large uncertainty about the estuarine contribution to the global N₂O budget. Incubation experiments with nitrogen stable isotope tracer (¹⁵N) were used to investigate the geochemical factors controlling N₂O production in the Chesapeake Bay, the largest estuary in North America. The highest potential rates of water column N₂O production (7.5±1.2 nmol-N L⁻¹ hr⁻¹) were detected during summer anoxia, during which oxidized nitrogen species (nitrate and nitrite) were absent from the water column. At the top of the anoxic layer, N₂O production from denitrification was stimulated by addition of nitrate and nitrite. The relative contribution of nitrate and nitrite to N₂O production was positively correlated with the ratio of nitrate to nitrite concentrations. Increased oxygen availability, up to 7 μM oxygen, inhibited both N₂O production and the reduction of nitrate to nitrite. In spring, high oxygen and low abundance of denitrifying microbes resulted in undetectable N₂O production from denitrification. Thus, decreasing the nitrogen input into the Chesapeake Bay has two potential impacts on the N₂O production: a lower availability of nitrogen substrates may mitigate short-term N₂O emissions during summer anoxia, and in the long-run (time scale of years), eutrophication will be alleviated and subsequent re-oxygenation of the bay will further inhibit N₂O production.

1 Introduction

Nitrous oxide (N₂O) is a strong greenhouse gas with 298-fold higher global warming potential per mole than that of carbon dioxide. N₂O is also a catalyst of ozone depletion in the stratosphere. Since the Industrial Revolution, the N₂O atmospheric concentration has been increasing at an unprecedented rate, and the current concentration is the highest in the last 800,000 years of Earth's history (Schilt et al., 2010). The contribution of N₂O emissions to global warming and ozone depletion will increase because N₂O is not as strictly regulated as are CO₂ and halocarbon compounds. With the successful mitigation of halocarbon compounds accomplished by the Montreal Protocol, N₂O is likely to be the single most important anthropogenically emitted ozone-depleting agent in the 21st century (Ravishankara et al., 2009).

29 Microbial processes are responsible for the majority of N₂O production, both in natural and anthropogenically impacted
30 environments. These pathways include oxidative and reductive processes occurring at the full range of environmental oxygen
31 concentrations. In the presence of oxygen, N₂O can be produced as a by-product during autotrophic aerobic ammonium (NH₄⁺)
32 oxidation to nitrite (NO₂⁻) by bacteria (Arp and Stein, 2003) and archaea (Santoro et al., 2011). The production of N₂O can
33 also occur via NO₂⁻ reduction by nitrifying organisms, termed nitrifier denitrification. This process was demonstrated in
34 cultures (Poeth and Focht, 1985; Frame and Casciotti, 2010), and in the water column of the subtropical North Pacific
35 Ocean (Wilson et al., 2014). Under low oxygen and anoxic conditions, [denitrifying bacteria](#) produce N₂O via enzyme-mediated
36 heterotrophic denitrification, which consists of the stepwise reduction of nitrate (NO₃⁻), NO₂⁻ and nitric oxide (NO), with
37 organic matter as the electron donor. [The *nirS* gene that encodes the genetic material for nitrite reductase \(the enzyme mediating
38 NO₂⁻ reduction to NO\) is often used as a proxy for abundance and diversity of denitrifying bacteria, and is the gene in the
39 denitrification sequence that is most reliably associated with a complete denitrification pathway \(Graf et al., 2014\).](#) N₂O is not
40 produced via anaerobic ammonium oxidation (anammox), another important nitrogen removal process in the natural
41 environment (Kartal et al., 2011).

42 The increase of atmospheric N₂O is attributed to intensification of human activities (e.g. fossil fuel combustion, fertilizer
43 application, human and animal waste disposal), which alter the microbial nitrogen cycle in the biosphere. Increased nitrogen
44 supply from fertilizer and atmospheric deposition causes increased N₂O emission not only from agricultural land, but also in
45 rivers, streams and coastal waters (Ciais et al., 2013; Thompson et al., 2014). Among these aquatic environments, intense N₂O
46 efflux originates from estuaries and associated river networks, which occupy 0.3% of global waters (Dürer et al., 2011) but
47 could contribute up to 10 % of anthropogenic fluxes (Seitzinger and Kroeze, 1998; Ciais et al., 2013). [Being the largest estuary
48 in the North America, the Chesapeake Bay and its tributaries have experienced eutrophication and expansion of summertime
49 anoxia due to increased population, expansion of industrialization and land use changes since the 18th century \(Cooper and
50 Brush, 1993; Boesch et al., 2001\). The Chesapeake tributary is a source of N₂O \(indicated by surface N₂O oversaturation\) in
51 the summertime between June and September \(Elkins et al., 1978; Kaplan et al., 1978; McElroy et al., 1978\). The summertime
52 water column is characterized by strong oxygen gradients \(equilibrium with atmosphere at the surface and complete anoxia
53 below ~ 10 m\), depletion of NO₃⁻ and NO₂⁻, and accumulation of NH₄⁺ in the deep water \(Lee et al., 2015b\). Increased microbial](#)

54 activities driving carbon assimilation and respiration have been demonstrated in the vicinity of the oxic-anoxic interface in the
55 water column (Lee et al., 2015a). However, the N₂O production pathway and the associated environmental controlling factors
56 have not been investigated.

57 Here we report a pilot study using nitrogen stable isotope (¹⁵N) incubation experiments to quantify N₂O production rates
58 and their dependence on the availabilities of oxygen, NO₃⁻ and NO₂⁻ in the Chesapeake Bay. Because seasonal anoxia occurs
59 at the study site in the central region of the Chesapeake Bay, reductive pathways of N₂O production (i.e. reduction of NO₃⁻ and
60 NO₂⁻) are the main focus. Further understanding of the environmental controls on N₂O production in estuaries will facilitate
61 the design of effective environmental engineering projects to mitigate N₂O emission.

62 **2 Methods**

63 **2.1 Sample acquisition and processing**

64 Sampling and incubation experiments were carried out on July 19, 2016, November 17, 2016 and May 3, 2017,
65 corresponding to typical conditions of summer, autumn and spring, respectively. Samples were collected at 38.55 °N, 76.43
66 °W (bottom depth 26.5 m) close to the mouth of the Choptank River in the central region of the Chesapeake Bay. Conductivity-
67 temperature-depth and oxygen were measured with a YSI sonde package (Model 600XLM with a 650 MDS display logger)
68 equipped with a diaphragm pump which was deployed for water sampling. The oxygen sensor had a detection limit of ~ 5
69 μmol L⁻¹. Samples for NO₂⁻ and NO₃⁻ concentration measurements were filtered (0.22 μm poresize, Sterivex-GP, EMD
70 Millipore) and frozen at -80 °C until analysis. Discrete samples for N₂O concentration were collected directly from the pump
71 outlet into the bottom of acid washed, 60 mL glass serum bottles (Catalog # 223745, Wheaton, Millville, NJ). Bottles were
72 sealed with butyl rubber stoppers (Catalog # W224100-202, Wheaton, Millville, NJ) and aluminium rings while submerged
73 under water pumped from depth to avoid atmospheric N₂O and oxygen contamination. Samples for characterizing N₂O
74 concentration profile were preserved immediately after filling by injecting 0.1 mL saturated HgCl₂. Samples for N₂O
75 incubation experiments (section 2.2) were acquired from 12 m, 17 m and 19.5 m during July 2016, November 2016 and May
76 2017, respectively, and sealed the same way as described above for discrete N₂O concentration samples, and stored in the dark
77 at 4 °C without adding HgCl₂. Samples for denitrifying *nirS* gene abundance were collected at 14, 17 and 19.5 m by filtering

78 600mL - 2000mL of water through 0.22 μm filter (Sterivex-GP, EMD Millipore) and frozen at $-80\text{ }^{\circ}\text{C}$ until DNA extraction
79 and analysis.

80 Samples for total dissolved inorganic carbon ($\text{DIC}=[\text{H}_2\text{CO}_3]+[\text{HCO}_3^-]+[\text{CO}_3^{2-}]$) and community respiration rates were
81 collected only in July 2016. The DIC samples were preserved with mercuric chloride (HgCl_2) for initial conditions, while
82 biochemical oxygen demand (BOD) bottles were incubated in a temperature-controlled environmental chamber ($\pm 1\text{ }^{\circ}\text{C}$ of in
83 situ water temperatures). After 24 h, samples were siphoned from the vials, preserved with HgCl_2 , and respiration rates were
84 determined as the difference in DIC between initial and final samples divided by 24 hours (Lee et al., 2015b).

85 2.2 ^{15}N incubation experiments for N_2O production

86 Within 3 hours of sampling, incubation experiments were initiated at the Horn Point Laboratory, Cambridge, Maryland.
87 Samples were divided into three sets for control, nitrogen manipulation and oxygen manipulation experiments.

88 Control experiment: The control experiment was conducted in July 2016, November 2016 and May 2017. A small (3
89 mL) headspace was created in the serum bottles, which were subsequently flushed with helium for 10 minutes to minimize
90 oxygen contamination from sampling and transportation. Two suites of ^{15}N tracer solutions ($^{15}\text{NO}_2^-$ plus $^{14}\text{NO}_3^-$, $^{15}\text{NO}_3^-$ plus
91 $^{14}\text{NO}_2^-$, 0.1mL) were injected to achieve final concentrations of $5\text{ }\mu\text{mol L}^{-1}$ NO_2^- and NO_3^- (see conditions for experiment 1-A
92 and 1-B, 4-A and 4-B, 6-A and 6-B in table 1). Tracer solutions were made from deionized water, and were flushed with
93 helium prior to addition to incubation experiments. In order to have enough mass to detect N_2O production, $\sim 1.2\text{ nmol}$ of
94 natural abundance N_2O was injected to each bottle, reaching a concentration of $\sim 20\text{ nmol L}^{-1}$ in the water phase (calculated
95 equilibrium concentration (Weiss and Price, 1980) with 3 mL headspace and 57 mL water). Initial conditions (one bottle for
96 each time course) were sampled within 30 minutes of tracer addition by injecting 0.1 mL saturated HgCl_2 . Incubations lasted
97 ~ 2 hours at *in situ* temperature ($\pm 0.5\text{ }^{\circ}\text{C}$), during which duplicate bottles were preserved with saturated HgCl_2 solution every
98 40 to 60 minutes, totalling seven bottles over four time points, including the initial for a time course analysis.

99 Dissolved inorganic nitrogen (DIN) manipulation: The DIN manipulation experiment was conducted only in July 2016
100 because NO_2^- and NO_3^- were absent from the water column (see section 3.1). A 3 mL headspace was created before flushing
101 with helium for 10 min to establish anoxic condition. Then, $\sim 1.2\text{ nmol}$ N_2O was injected to reach a concentration of $\sim 20\text{ nmol}$
102 L^{-1} in the water phase. Two suites of ^{15}N tracer solutions ($^{15}\text{NO}_2^-$ plus $^{14}\text{NO}_3^-$, $^{15}\text{NO}_3^-$ plus $^{14}\text{NO}_2^-$, 0.1 mL of total volume of

103 tracer addition) were injected to designated bottles to achieve ratios of $\text{NO}_2^- : \text{NO}_3^- \approx 1:10, 1:3, 3:1$ and $10:1$, with ^{15}N fraction
104 labelled between 0.016 and 0.16 (Table 1, experiment 2-A to 2-H). This allows simultaneous detection of N_2O production
105 from NO_2^- and NO_3^- at different ratios of NO_2^- to NO_3^- concentration. Incubations lasted ~ 2 hours with the same sampling
106 strategy as the control experiment.

107 Oxygen manipulation: The oxygen manipulation experiment was conducted in July 2016 and November 2016.
108 Headspace (3 – 8 mL) was created before flushing with helium for 10 minutes. Oxygen-saturated site water was made by air-
109 equilibration at *in situ* temperature. To achieve different oxygen levels, 0.2, 0.5, 1.0, 2.0 or 5.0 mL of oxygen-saturated site
110 water was injected. With a final volume of ~3 mL of headspace during the course of the incubation, the oxygen concentrations
111 in the water phase were 0.3 to 6.4 $\mu\text{mol L}^{-1}$ in July 2016 (Table 1, experiment 3-A – 3-J), and were 0.2 to 7.3 $\mu\text{mol L}^{-1}$ in
112 November 2016 (Table 1, experiment 5-A – 5-J) after the calculated equilibration between headspace and seawater (Garcia
113 and Gordon, 1992). In addition, an optical sensor was used to measure oxygen concentrations directly in a parallel experimental
114 setup and the agreement between calculated target concentration and measured concentration was excellent (data not shown).
115 After oxygen adjustment, ~1.2 nmol N_2O was injected into each bottle, and two suites of ^{15}N tracer solutions ($^{15}\text{NO}_2^-$ plus
116 $^{14}\text{NO}_3^-$, $^{15}\text{NO}_3^-$ plus $^{14}\text{NO}_2^-$, 0.1 mL) were injected to achieve final concentration of 5 $\mu\text{mol L}^{-1}$ NO_2^- and NO_3^- . The ^{15}N fraction
117 for NO_2^- or NO_3^- during the incubation experiments are shown in Table 1. Incubations lasted ~ 2 hours with the same sampling
118 strategy as the control experiment.

119 2.3 Analytical procedures

120 For water column nutrients, dissolved NO_2^- was measured using a colorimetric method (Hansen and Koroleff, 2007) and
121 $\text{NO}_3^- + \text{NO}_2^-$ was measured using a hot (90 °C) acidified vanadium (III) reduction column coupled to a chemiluminescence
122 NO/NO_x Analyzer (Teledyne API, San Diego, CA) (Garside, 1982; Braman and Hendrix, 1989). DIC was measured with an
123 automated infrared analyzer (Apollo SciTech, Newark, DE) as previously reported (Lee et al., 2015b). Preserved N_2O samples
124 were stored in the dark at room temperature (~22 °C) for less than three weeks before analysis. Dissolved N_2O was extracted
125 by flushing with helium for 40 min at a rate of 37 mL min⁻¹ (extraction efficiency $99 \pm 2\%$), and subsequently cryo-trapped
126 by liquid nitrogen and isolated from interfering compounds (H_2O , CO_2) by gas chromatography (Weigand et al., 2016). Pulses
127 of purified N_2O were injected into a Delta V^{Plus} mass spectrometer (Thermo Fisher Scientific, Waltham, MA) for mass ($m/z =$

128 44, 45, 46) and isotope ratio ($m_1/m_2 = 45/44, 46/44$) measurements. The amount of N_2O was calibrated with standard N_2O
129 vials, which were made by injecting 1, 2, or 5 nmol N_2O-N into 20 mL glass vials (Catalog # C4020-25, Thermo Fisher
130 Scientific, Waltham, MA).

131 After N_2O analysis, samples incubated with $^{15}NO_3^-$ were also assayed for $^{15}NO_2^-$ to determine rates of NO_3^- reduction.
132 Two millilitres of each sample were transferred from the 60-mL serum bottle to a 20-mL glass vial and then flushed with
133 helium for 10 min. Dissolved $^{15}NO_2^-$ was converted to N_2O using the acetic acid-treated sodium azide solution for quantitative
134 conversion (McIlvin and Altabet, 2005). Resulting N_2O was measured on the Delta V^{Plus} for nitrogen isotope ratio so as to
135 determine the ^{15}N enrichment of NO_2^- .

136 For the analysis of *nirS* gene abundance, DNA extraction and qPCR for the *nirS* gene using SYBR Green were performed
137 as previously described (Jayakumar et al. 2009; 2013). Extracted DNA was quantified using PicoGreen fluorescence
138 (Molecular Probes, Eugene, OR) prior to the qPCR assay. Samples for qPCR were run in triplicates including a no template
139 control, a no Primer control and 5 different dilutions of a *nirS* standard. Threshold cycle (Ct) values were obtained using
140 automatic analysis settings of the quantitative PCR and further used to calculate the gene copy numbers as described in
141 Jayakumar et al. (2013).

142 2.4 Data analysis

143 N_2O concentration was calculated from the amount of N_2O detected by mass spectrometry divided by the volume of
144 water in the serum bottles. N_2O production (R) was calculated from the progressive increase in $^{45}N_2O$ and $^{46}N_2O$ concentrations
145 in each serum bottle over the time course experiments.

$$146 R = \frac{1}{F} \times \left(\frac{d^{45}N_2O}{dt} + 2 \times \frac{d^{46}N_2O}{dt} \right) \quad (1)$$

147 where $d^{45}N_2O/dt$ and $d^{46}N_2O/dt$ represent the production rates ($nmol-N L^{-1} hr^{-1}$) of mass 45 and 46 N_2O during incubation. F
148 represents the ^{15}N fraction in the initial substrate (NO_2^- or NO_3^-). Rates were considered significant based on the linear
149 regression of the time course data ($p < 0.05, n=7$, student t-test). The detection limit for N_2O production is $0.002 nmol-N L^{-1}$
150 hr^{-1} . The ^{15}N incubation experiments can identify the pathway but cannot distinguish the relative contributions of two or more

151 functioning microbial groups to a single N₂O production pathway (i.e. N₂O production via NO₂⁻ reduction by nitrifier
152 denitrification and/or heterotrophic denitrification).

153 The rate of NO₃⁻ reduction to NO₂⁻ was calculated as

$$154 \text{ NO}_2^- \text{ production} = (d^{15}\text{NO}_2^-/dt) / F \quad (2)$$

155 where $d^{15}\text{NO}_2^-/dt$ represents the production rate of ¹⁵NO₂⁻ (nmol-N L⁻¹ hr⁻¹), which is calculated as the slope of ¹⁵NO₂⁻
156 concentrations versus time. F represents initial substrate ¹⁵NO₃⁻ enrichment. Rates were considered significant based on linear
157 regression of the time course data ($p < 0.05$, student's t -test). The detection limit for NO₂⁻ production is 0.05 nmol-N L⁻¹ hr⁻¹.

158

159 **3 Results and discussion**

160 **3.1 Water column features**

161 The physical and chemical properties of the water column in central Chesapeake Bay experience seasonal variation (Fig.
162 1). Temperature and salinity differed among the three seasons but were essentially constant in the top 7 m of the water column
163 on the three sampling dates. In July, the water column was stratified because of lower salinity (~ 16 PSU) and higher
164 temperature (~ 28.5 °C) in the top ~ 10 m resulting in a pronounced halocline and thermocline (Fig. 1a and 1b). Less
165 pronounced stratification in May and November was due to a weaker temperature difference between the top 10 m and below.
166 The July oxygen profile showed a significant concentration decrease between 3 to 10 m (Fig. 1c), with a sharp oxycline (~ 30
167 μmol L⁻¹ m⁻¹). Below 10 m, the oxygen concentration was below detection of the sensor (~ 5 μmol L⁻¹) and was likely anoxic.
168 However, sulphide compounds were most likely not present in July at depth; the water samples were free of any hydrogen
169 sulphide odor. No anoxic layer was observed in May and November (Fig. 1c), and previous studies showed that the water
170 column of the Chesapeake Bay was reoxygenated following summertime anoxia during winter and spring (Lee et al., 2015a).

171 The surface N₂O saturation values in July, November and May were 6.6, 10.4 and 12.0 nmol L⁻¹, respectively. In July,
172 N₂O concentration was close to air-saturation level (6.6 nmol L⁻¹) at the surface layer. In the low oxygen layer (below 12 m),
173 N₂O was apparently undersaturated (2.0 – 3.7 nmol L⁻¹, 20 – 50 % air-saturation, Fig. 1d). In November, the surface N₂O
174 concentration was slightly oversaturated (11.3 nmol L⁻¹, 108 % air-saturation). N₂O concentrations at depth were oversaturated;
175 the concentrations varied between 11.0 and 11.5 nmol L⁻¹, corresponding to 109 – 115 % air-saturation. In May, both the

176 surface and water column N₂O concentrations were air-undersaturated; the surface concentration was 9.1 nmol L⁻¹, 76 % air-
177 saturation; concentrations between 8 and 17 m ranged from 9.4 to 11.0 nmol L⁻¹, corresponding to 82 – 97 % air-saturation.
178 As the surface and water column N₂O saturation levels vary greatly between seasons; the assessment of the N₂O dynamics of
179 the Chesapeake Bay requires expanding the temporal and spatial coverage of the field sampling. In the following, we focus on
180 N₂O production and its environmental controlling factors.

181 The concentrations of NO₃⁻ and NO₂⁻ (Fig. 1e and 1f) in July were below 0.02 μmol L⁻¹ within the sampling depth interval
182 (top 17 m of water column). Measureable levels of NO₃⁻ and NO₂⁻ species were found in May and November. The surface
183 concentrations of NO₃⁻ and NO₂⁻ in May were 20 and 0.5 μmol L⁻¹, respectively; and the concentrations decreased with depth.
184 In November, NO₃⁻ and NO₂⁻ were depleted at the surface (~ 3 m) and their concentrations increased with depth; at 17 m the
185 concentrations of NO₃⁻ and NO₂⁻ were 5.0 and 0.4 μmol L⁻¹, respectively. The increase of water column NO₃⁻ and NO₂⁻
186 concentrations was likely due to increased runoff from the anthropogenically influenced watershed. Water column depletion
187 of NO₃⁻ and NO₂⁻ in the summer is the result of denitrification (Baird et al., 1995; Boynton et al., 1995), which indicates
188 potential water column N₂O production via denitrification (discussed in section 3.2).

189 As a proxy for the size of the denitrifying community, the abundance of the *nirS* gene was $(5.91 \pm 0.1) \times 10^4$ copy mL⁻¹
190 at 14 m in July, which was the highest among the three sampling trips (Fig. 1g). Lowest *nirS* gene abundance $(9.1 \pm 1.3) \times 10^3$
191 copy mL⁻¹ was observed in May at 19.5 m. The abundance of *nirS* was measured only at the depths at which incubations were
192 performed, and the *nirS* abundance increased with increasing rates of N₂O production (see section 3.2). In July 2016, water
193 column DIC concentrations ranged from 1,377 to 1,831 μmol L⁻¹, with the highest concentrations below 10 m. Average
194 community respiration rates at 3 m and 14 m depth were 2.01 and 0.63 μmol L⁻¹ hr⁻¹, respectively.

195 **3.2 Active water column N₂O production**

196 The anoxic control experiment (anoxic condition with 5 μmol L⁻¹ NO₂⁻ or NO₃⁻) was used to demonstrate active N₂O
197 production: In July 2016, at the top of anoxic layer (~ 12.3 m), rates of N₂O production from NO₂⁻ and NO₃⁻ reduction were
198 5.42 ± 0.35 and 2.04 ± 0.86 nmol-N L⁻¹ hr⁻¹, respectively (Fig. 2). In November 2016, at 17 m within the oxygenated water
199 column ([O₂] > 180 μmol L⁻¹), rates of N₂O production were 0.33 ± 0.01 and 0.95 ± 0.35 nmol-N L⁻¹ hr⁻¹, respectively. In May
200 2017, no N₂O production was detected at 19.5 m.

201 The total N₂O production rate of 7.5 ± 1.2 nmol-N L⁻¹ hr⁻¹ in July 2016 is lower than the measurements (18 – 77 nmol-N
202 L⁻¹ hr⁻¹) made 40 years ago in the Potomac River (McElroy et al., 1978), a tributary to the Chesapeake Bay. This difference
203 could be due to much higher water column nutrients in the Potomac River (NO₂⁻ plus NO₃⁻ concentration > 30 μmol L⁻¹) at
204 that time, and presumably denser microbial populations because of sediment resuspension (4 – 10 m water depth). With added
205 substrates (NO₂⁻ and NO₃⁻) being more than an order of magnitude higher than *in situ* levels in July 2016, and the anoxic
206 conditions being used in the November 2016 experiments (in situ [O₂] > 180 μmol L⁻¹), N₂O production rates reported here
207 are potential rates, which nevertheless highlight the potential for N₂O production in anoxic waters responding rapidly (within
208 hours) to pulses of NO₂⁻ or NO₃⁻.

209 Based on the *nirS* gene abundance, the denitrifying population was more abundant in July (summer) than November
210 (autumn), and was the smallest in May (spring) in the lower water column (14 – 19.5 m) of the Chesapeake Bay (Fig. 1g). In
211 July highest N₂O production rates co-occurred with the highest *nirS* abundances (Fig. 2). While the water column oxygen in
212 November was > 180 μmol L⁻¹, the *nirS* gene abundance supported potential denitrification at a N₂O production rate of $1.28 \pm$
213 0.35 nmol-N L⁻¹ hr⁻¹ in anoxic incubation experiments. In May when hypoxic conditions had not yet developed, no N₂O
214 production was detected, and the *nirS* abundance (9.1×10^3 copies mL⁻¹) was the lowest among three sample dates. **It is likely**
215 **that the denitrifying community did not recover from oxygen inhibition during the 2-hour anoxic incubation.** A
216 metatranscriptome analysis showed that the transcript ratios for denitrification were the lowest in June before the onset of
217 hypoxia, and highest ratios in August when anoxia was most pronounced (Eggleston et al., 2015).

218 3.3 N₂O production pathways regulated by availability of nitrogen substrate

219 The ratio of the rates of N₂O production from NO₂⁻ reduction vs. N₂O production from NO₃⁻ reduction positively
220 correlates with the ratio of NO₂⁻ : NO₃⁻ concentrations (Fig. 3). This suggests **increasing NO₂⁻ or NO₃⁻ availability favours N₂O**
221 **production from the reduction of the respective substrate.** At concentration ratios of NO₂⁻ : NO₃⁻ < 0.5, the ratios of rates were
222 similar to the concentration ratio, 0.3 ± 0.2 . At a concentration ratio of NO₂⁻ : NO₃⁻ = 1 : 1, the ratio of rates of N₂O production
223 from respective substrates measured from replicate experiments varied from 0.6 to 2.6. At NO₂⁻ : NO₃⁻ = 10, the ratio of rates
224 was greater than 10. Therefore, the primary nitrogen source of N₂O production via denitrification depends in part on the relative
225 availability of the substrate (NO₂⁻ or NO₃⁻).

226 As denitrification is a step-wise enzymatic reduction from NO_3^- , NO_2^- , NO , N_2O to N_2 , the pathway can be somewhat
227 modular (Graf et al., 2014), i.e., many organisms possess only one or a few steps, rather than the complete pathway. In complete
228 denitrifiers (organisms capable of reducing NO_3^- to N_2), the degree to which intermediates (i.e. NO_2^-) exchange across cellular
229 membranes with the ambient environment is unknown (Moir and Wood, 2001). We use data from the DIN manipulation
230 experiment (conducted in July 2016) to show that full exchange between intracellular and ambient NO_2^- during NO_3^- reduction
231 to N_2O is unlikely, as explained below.

232 The conditions and results from experiment 2-H (Table 1) were used because this experiment had the highest ambient
233 NO_2^- pool and an exchange between the pools could be easily detected. During NO_3^- reduction to N_2O , if denitrifiers reduce
234 $^{15}\text{NO}_3^-$ (total $1.2 \mu\text{mol L}^{-1}$, ^{15}N fraction labeled 0.16) to $^{15}\text{NO}_2^-$ at maximal rate ($0.2 \mu\text{mol-N L}^{-1} \text{ hr}^{-1}$, see section 3.4) and the
235 product fully exchanges with the ambient $^{14}\text{NO}_2^-$ ($10 \mu\text{mol L}^{-1}$, ^{15}N fraction labeled 0.0037), after 2 hours, the ^{15}N addition to
236 the total NO_2^- pool will be $0.064 \mu\text{mol L}^{-1}$:

237 (Rate of NO_2^- production from NO_3^- \times incubation time \times initial fraction labelled of NO_3^-)

238 = $(0.2 \mu\text{mol-N L}^{-1} \text{ hr}^{-1} \times 2 \text{ hr} \times 0.16) = 0.064 \mu\text{mol L}^{-1}$,

239 and the resulting ^{15}N fraction (unitless) of NO_2^- will be 0.01:

240 (^{15}N addition to NO_2^- + initial fraction labelled of NO_2^- \times initial concentration of NO_2^-) / (total concentration of NO_2^-)

241 = $(0.064 \mu\text{mol L}^{-1} + 0.0037 \times 10 \mu\text{mol L}^{-1}) / (10 + 0.064) \mu\text{mol L}^{-1} \approx 0.01$.

242 Assuming $6 \text{ nmol-N L}^{-1} \text{ hr}^{-1}$ as the rate of N_2O production from NO_2^- reduction (the $\text{NO}_2^- \rightarrow \text{N}_2\text{O}$ rate shown in fig. 3; ^{15}N
243 fraction labeled of $\text{NO}_2^- = 0.01$), and the initial N_2O concentration as 20 nmol L^{-1} (described in section 2.2; ^{15}N fraction labeled
244 of $\text{N}_2\text{O} = 0.0037$), after 2 hours, the resulting ^{15}N fraction of N_2O will be 0.0052:

245 (^{15}N fraction labelled of NO_2^- \times rate of N_2O production from NO_2^- \times incubation time) + (initial fraction labelled of N_2O \times initial
246 concentration of N_2O \times molar nitrogen in molar N_2O) / ((rate of N_2O production from NO_2^- \times incubation time) + (initial
247 concentration of N_2O \times molar nitrogen in molar N_2O))

248 $= ((0.01 \times 6 \text{ nmol-N L}^{-1} \text{ hr}^{-1} \times 2 \text{ hr}) + (0.0037 \times 20 \text{ nmol-N}_2\text{O L}^{-1} \times 2\text{N/N}_2\text{O})) / (6 \times 2 + 20 \times 2) \text{ nmol-N L}^{-1} = 0.0052$

249 The calculated ^{15}N fraction of N_2O (0.0052) is much lower than the measured ^{15}N fraction of N_2O (> 0.02) in experiment 2H.
250 This means that full exchange of NO_2^- during NO_3^- reduction to N_2O , at maximum possible rates of NO_3^- reduction to NO_2^-
251 and N_2O , would yield a rate of N_2O production from NO_3^- much lower than observed in the experimental results. Thus, we
252 concluded that the intracellular exchange of NO_2^- during NO_3^- reduction to N_2O by the denitrifying community in Chesapeake
253 Bay is limited. Such a tight coupling among nitrate reduction, nitrite reduction and nitric oxide reduction suggests the co-
254 occurrence of the respective functional genes and enzymes in the cell of nitrate reducers. Both dissimilatory nitrate and nitrite
255 reducers are able to produce N_2O independently, so total N_2O production can be quantified accurately by separate measurement
256 of NO_3^- and NO_2^- reduction.

257 **3.4 Oxygen inhibits N_2O production by denitrification**

258 The sensitivities to increasing $[\text{O}_2]$ of NO_2^- reduction and NO_3^- reduction to N_2O were evaluated in samples from July
259 and November 2016 (Fig. 4). The control experiment (anoxic incubation, see Section 3.2) showed a total N_2O production rate
260 (from NO_2^- plus NO_3^- reduction) of 7.5 ± 1.2 and $1.28 \pm 0.35 \text{ nmol-N L}^{-1} \text{ hr}^{-1}$ during July 2016 and November 2016, respectively.
261 Increasing $[\text{O}_2]$ generally decreased N_2O production rates from denitrification. In July 2016, under $[\text{O}_2] = 0.3 \text{ } \mu\text{mol L}^{-1}$, N_2O
262 production from NO_2^- reduction decreased from 5.4 to 2.5 $\text{nmol-N L}^{-1} \text{ hr}^{-1}$, whereas the rate of NO_3^- reduction to N_2O increased
263 from 2.0 to 3.5 $\text{nmol-N L}^{-1} \text{ hr}^{-1}$. Further increase in $[\text{O}_2]$, up to 6.4 $\mu\text{mol L}^{-1}$, significantly inhibited the rate of N_2O production
264 from both NO_2^- and NO_3^- reduction (Fig. 4a). Note that 6 $\mu\text{mol L}^{-1}$ $[\text{O}_2]$ did not fully inhibit N_2O production from NO_2^-
265 reduction, the rate of which was 0.08 $\text{nmol-N L}^{-1} \text{ hr}^{-1}$. However, N_2O production from NO_3^- reduction was completely inhibited
266 when $[\text{O}_2] > 0.6 \text{ } \mu\text{mol L}^{-1}$. Similar to results from July 2016, in November 2016, increasing $[\text{O}_2]$ gradually decreased rates of
267 NO_2^- reduction to N_2O ; no rates were detected when $[\text{O}_2] > 2 \text{ } \mu\text{mol L}^{-1}$. Rates of NO_3^- reduction to N_2O were not detected at
268 $[\text{O}_2] > 0 \text{ } \mu\text{mol L}^{-1}$ (Fig. 4b).

269 Rate of NO_3^- reduction to NO_2^- was also measured in July 2016 to supplement the sensitivity analysis of denitrification
270 to oxygen. The rate of NO_3^- reduction to NO_2^- was 100 $\text{nmol L}^{-1} \text{ hr}^{-1}$ under anoxic condition. At $[\text{O}_2] = 0.3 \text{ } \mu\text{mol L}^{-1}$, the rate

271 doubled, to 200 nmol-N L⁻¹ hr⁻¹ (Fig. 4). Further increase of [O₂] significantly decreased the rate of NO₃⁻ reduction to NO₂⁻.
272 However, at [O₂] = 6.4 μmol L⁻¹ NO₃⁻ reduction to NO₂⁻ was still detectable at 0.82 ± 0.06 nmol-N L⁻¹ hr⁻¹ (Fig. 5).

273 These results suggest that oxygenation of the water column in the Chesapeake Bay, even micro-molar level oxygen,
274 would significantly mitigate N₂O production. Both July 2016 and November 2016 data showed the difference in the effect of
275 oxygen on N₂O production from NO₂⁻ vs. NO₃⁻ reduction. Samples from July 2016 showed 98% and complete inhibition on
276 N₂O production from NO₂⁻ and NO₃⁻ reduction at [O₂] = 6 μmol L⁻¹, respectively. The November 2016 samples showed 94 %
277 and complete inhibition on N₂O production from NO₂⁻ and NO₃⁻ reduction at [O₂] = 0.4 μmol L⁻¹, respectively. **Furthermore,**
278 **N₂O production in the Chesapeake Bay was likely attributed to both heterotrophic denitrification and nitrifier denitrification.**
279 Studies have shown that both nitrifiers and denitrifiers are present in the Chesapeake Bay (Bouskill et al., 2012; Hong et al.,
280 2014) and they are capable of NO₂⁻ reduction to N₂O, whereas NO₃⁻ reduction to N₂O is solely mediated by heterotrophic
281 denitrifiers. N₂O production via nitrifier denitrification occurs under the full range of oxygen environments in agricultural
282 soil (Zhu et al., 2013) and the open ocean (Wilson et al., 2014). Partial denitrification (NO₃⁻ reduction to N₂O) however, is
283 moderately oxygen sensitive. Thus, increasing oxygen inhibits the activities of denitrifiers, as demonstrated in decreasing rates
284 of NO₃⁻ reduction to N₂O (Fig. 3) and NO₃⁻ reduction to NO₂⁻ (Fig. 5). Increasing oxygen does not completely inhibit N₂O
285 production activity of nitrifiers but probably lowers the N₂O production rates by nitrifier denitrification.

286 **4 Conclusion and outlook**

287 The Chesapeake Bay is a potential N₂O source via denitrification when NO₃⁻ and NO₂⁻ are present **under anoxic**
288 **conditions. Relative rates of NO₃⁻ and NO₂⁻ reduction to N₂O were positively correlated with relative concentrations of NO₃⁻**
289 **and NO₂⁻. Increased oxygen availabilities, either by natural water column oxygenation or by experimental manipulation, caused**
290 **decreased N₂O production rates via denitrification. The size of the denitrifying community increased with increasing rates of**
291 **N₂O production via denitrification. The potential N₂O production in the summertime suggests that intermittent N₂O efflux to**
292 **the atmosphere could occur when a shallow oxic-anoxic interface (typically 10 – 15 m) is present (Taft et al., 1980; Kemp et**
293 **al., 1992; Lee et al., 2015a), and frequent disturbance of water column stratification by storm events, boat traffic and surface**
294 **cooling. The seasonal variation of surface and water column N₂O saturation levels (air-undersaturated in May and air-**

295 oversaturated in November), and the detection of significant N₂O production in July (summer) when N₂O concentrations were
296 the lowest imply that N₂O consumption was also occurring in the Chesapeake Bay and probably minimizing N₂O efflux to the
297 atmosphere. A long-term, comprehensive survey with wide spatial coverage will help assess if the Chesapeake Bay is a net
298 N₂O source or sink on an annual scale, and to investigate the physical, chemical and biological controls of N₂O emission in
299 the Chesapeake Bay.

300 Denitrification is critical for complete removal of fixed nitrogen so as to mitigate eutrophication in natural waters. The
301 N₂O production rates could serve as a proxy for estimating nitrogen loss. It is estimated that 1% of total denitrified nitrogen is
302 converted to N₂O in river networks (Beaulieu et al., 2011) so the ratio of N₂O : N₂ during denitrification = 1 : 100. Assuming
303 that N₂O production occurs at a rate of 7 nmol-N L⁻¹ hr⁻¹ within 0.2 m of the oxic-anoxic interface in summertime (based on
304 the July 2016 control data, N₂O production from NO₃⁻ plus NO₂⁻), denitrification yields a potential water column N removal
305 rate of 140 μmol-N m⁻² hr⁻¹, or 0.24 mg-N m⁻² d⁻¹. In addition, the sediment in the Bay is capable of anaerobic ammonia
306 oxidation (Rich et al., 2008) and denitrification (Kemp et al., 1990; Kana et al., 2006). Total sedimentary N₂ production,
307 measured by the acetylene block reduction method (Kemp et al., 1990) and N₂ accumulation method (Kana et al., 2006)
308 recorded areal rates of 50 – 70 μmol-N m⁻² hr⁻¹. Therefore, the sediment-water system in the Chesapeake Bay is effective in
309 biological nitrogen removal.

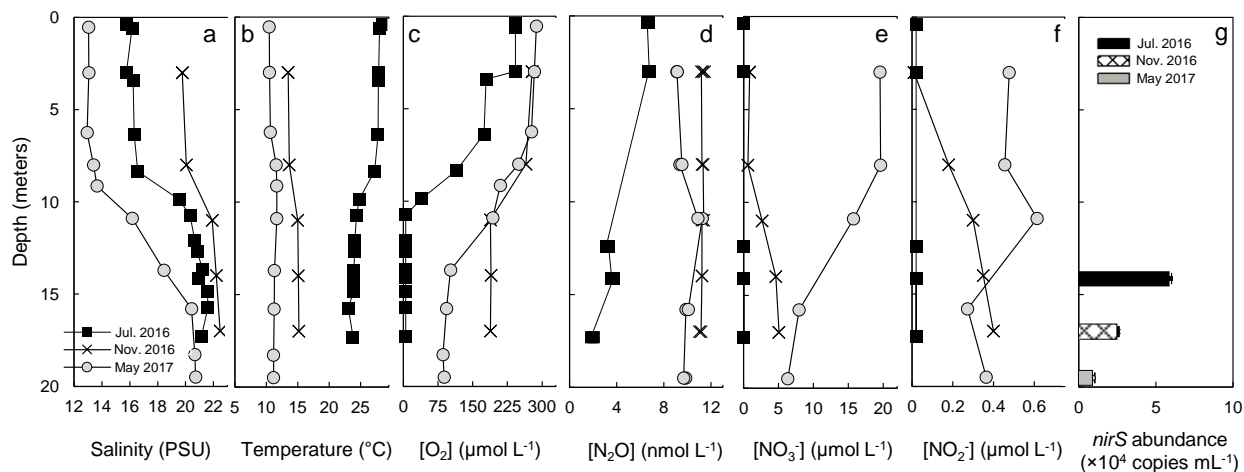
310 The oxidation of NH₄⁺, *although not the focus of this study*, is a possible pathway for N₂O production under low oxygen
311 conditions (Anderson, 1964). The yield of N₂O (molar ratio of N₂O production to NH₄⁺ oxidation) increases with decreasing
312 oxygen (Goreau et al., 1980). Culture (Qin et al., 2017) and field studies (Bristow et al., 2016; Peng et al., 2016) have shown
313 high affinity of oxygen (< 5 μmol L⁻¹) during NH₄⁺ oxidation. The main sources of NH₄⁺ in the Chesapeake Bay include
314 remineralization of organic matter in the oxygenated water column and sediments (Kemp et al., 1990) and atmospheric
315 deposition (Larsen et al., 2001). Onset of NH₄⁺ oxidation is viable at NH₄⁺ concentration < 100 nmol L⁻¹ by the natural
316 ammonia oxidizing community (Horak et al., 2013). Thus, N₂O production from NH₄⁺ oxidation might be stimulated under
317 low oxygen conditions by influx of ammonium near the oxic-anoxic interface, which deserves future research efforts.

318 The inhibition of N₂O production by oxygen highlights the positive outcomes of re-oxygenation of the Chesapeake Bay.
319 Since the late 20th century, Chesapeake Bay has received increased anthropogenic nitrogen loading from various sources

320 including fertilizer (Groffman et al., 2009), untreated sewage (Kaplan et al., 1978) and atmospheric deposition (Russell et al.,
321 1998; Loughner et al., 2016). Fueled by increased nitrogen input, elevated primary production in the surface layer stimulates
322 aerobic remineralization at depth, which consumes oxygen rapidly. In summertime, water column stratification restricts influx
323 of oxygen to depth, creating seasonal anoxia/hypoxia in the Bay. The documented eutrophication and expansion of
324 anoxia/hypoxia in the Chesapeake Bay in the late 20th century attracted public attention because of increasing mortality of
325 organisms with high commercial and recreational value (Cooper and Brush, 1993). Moreover, expansion of the volume of low
326 oxygen waters will result in more “hot spots” for N₂O production. The key factor of mitigating anoxia is to control the nitrogen
327 input to the bay (Hagy et al., 2004; Zhou et al., 2014). Effective fertilizer application, sewage treatment, natural nitrogen
328 removal by denitrification/anammox, and plant uptake have been successfully enforced to control the nitrogen runoff into the
329 bay from the tributaries (Boesch et al., 2001; Program, 2017). The near absence of summertime water column NO₂⁻ + NO₃⁻
330 concentrations near the middle of Chesapeake Bay as shown in this study and others (Lee et al., 2015a) could prevent N₂O
331 production. Reducing the nitrogen input into the Chesapeake Bay will help mitigate N₂O efflux: In the short-term (time scale
332 of days to months), nitrogen sources (NH₄⁺, NO₂⁻ and NO₃⁻) for N₂O production will be decreased. In the long run (inter-annual
333 time scale), eutrophication will be alleviated, which will re-oxygenate the water column, and inhibit N₂O production.

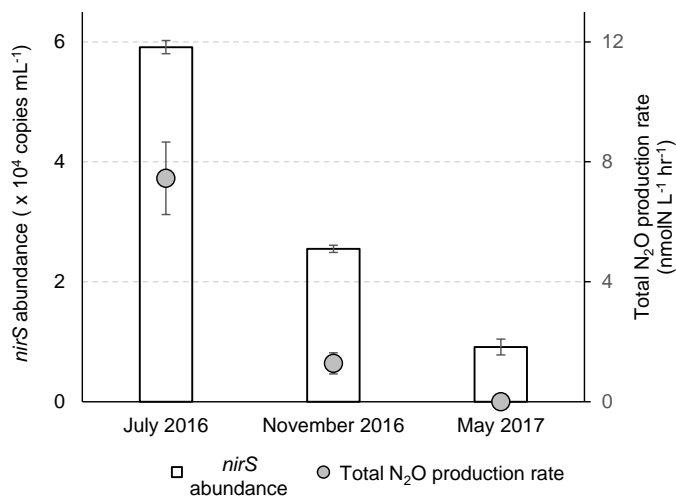
334

335



336

337 **Figure 1: Depth profiles on three sampling dates, July 19, 2016 (filled square), November 17, 2016 (cross), May 3, 2017 (grey circle)**
 338 **of a) salinity, b) temperature, c) oxygen, d) nitrous oxide, e) nitrate, f) nitrite. Analysis of *nirS* gene abundance (g) was only conducted**
 339 **at one depth, at which incubations were also performed, during each trip.**

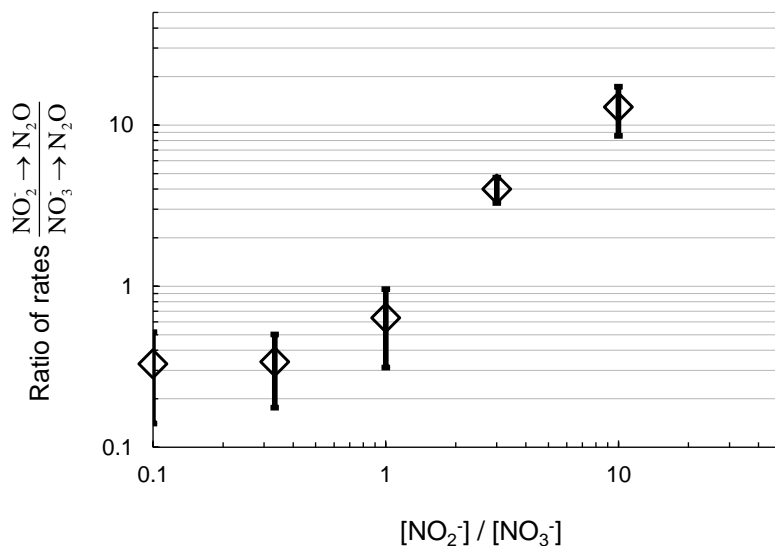


340

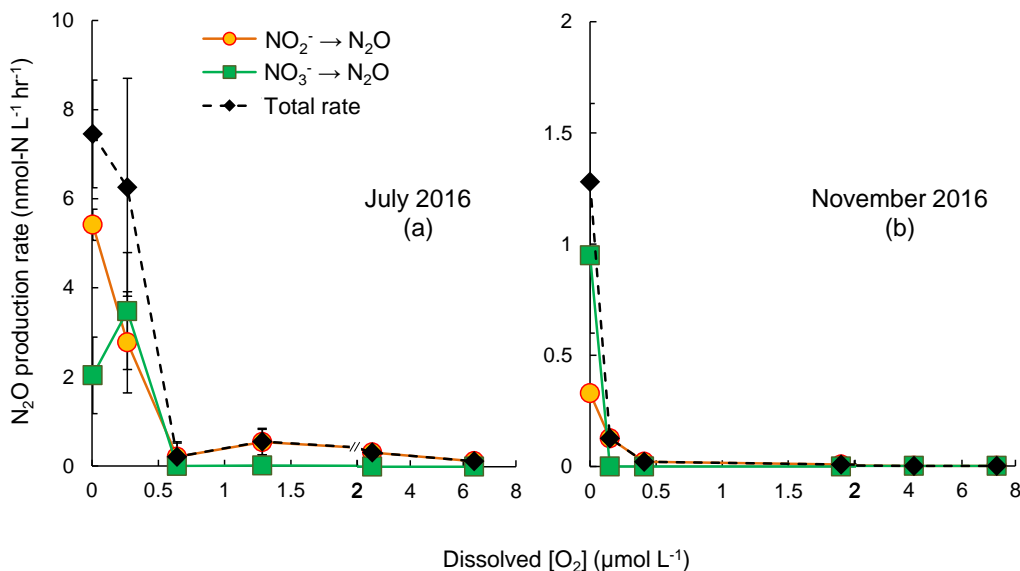
341 **Figure 2: Abundances of *nirS* gene and total N₂O production rates (from nitrate plus nitrite reduction) at three sampling times. The**
 342 ***nirS* gene abundances were analyzed at 14.1, 17.0 and 19.5 m during July 2016, November 2016 and May 2017, respectively. The**
 343 **total N₂O production rates were measured in the control experiment (helium-flushed anoxic incubation) at 12.3, 17.0 and 19.5 m**
 344 **during July 2016, November 2016 and May 2017, respectively.**

345

346

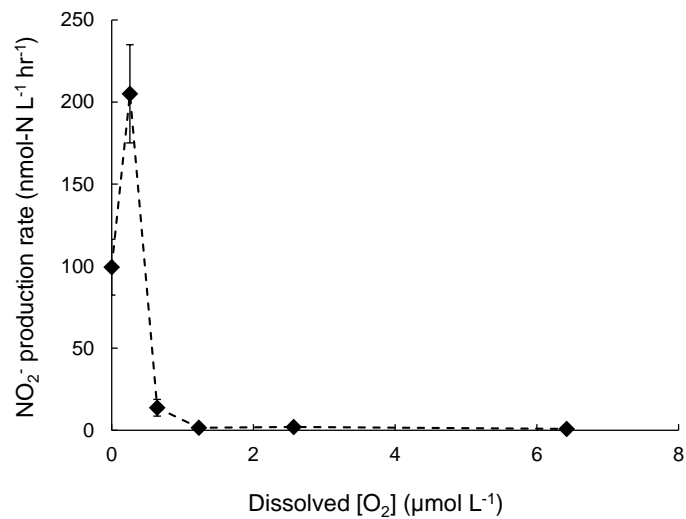


347
 348 **Figure 3: Ratio of rates of N₂O production from NO₂⁻ reduction and NO₃⁻ reduction plotted with the respective ratio of NO₂⁻ to**
 349 **NO₃⁻ concentration in the DIN manipulation experiment from July 2016 sampling. Log scale on both axes is for clarity at the low**
 350 **values.**
 351



352
 353 **Figure 4: Rates of N₂O production from NO₂⁻ reduction (orange circles), NO₃⁻ reduction (green squares) and combined NO₂⁻ and**
 354 **NO₃⁻ reduction (black diamonds) under increasing oxygen concentrations in July 2016 (a) and November 2016 (b). The standard**
 355 **deviation of rates in most of the samples were small so that error bars are not visible. Note the scale break at 2 µmol L⁻¹ O₂ on x-**
 356 **axis.**

357
358



359
360
361

Figure 5: Rates of NO₂⁻ production from NO₃⁻ reduction under increasing oxygen concentrations. Error bar indicates the standard deviation of rates from linear regression of three time points (n=7).

362

Experiment	Experiment ID	¹⁵ NO ₂ ⁻ (μM)	¹⁵ NO ₃ ⁻ (μM)	¹⁴ NO ₂ ⁻ (μM)	¹⁴ NO ₃ ⁻ (μM)	NO ₂ ⁻ :NO ₃ ⁻	¹⁵ N fraction label (species)	O ₂ (μM)
Control (July 2016)	1-A	5			5	1:1	0.99 (NO ₂ ⁻)	0
	1-B		5	5		1:1	0.99 (NO ₃ ⁻)	0
Nitrogen manipulation (July 2016)	2-A	0.2		1	10	1.2 : 10	0.16 (NO ₂ ⁻)	0
	2-B		0.2	1	10	1 : 10.2	0.016 (NO ₃ ⁻)	0
	2-C	0.2		1	3	1.2 : 3	0.16 (NO ₂ ⁻)	0
	2-D		0.2	1	3	1 : 3.2	0.06 (NO ₃ ⁻)	0
	2-E	0.2		3	1	3.2 : 1	0.06 (NO ₂ ⁻)	0
	2-F		0.2	3	1	3 : 1.2	0.16 (NO ₃ ⁻)	0
	2-G	0.2		10	1	10.2 : 1	0.016 (NO ₂ ⁻)	0
	2-H		0.2	10	1	10 : 1.2	0.16 (NO ₃ ⁻)	0
Oxygen manipulation (July 2016)	3-A	5			5	1:1	0.99 (NO ₂ ⁻)	0.3
	3-B		5	5		1:1	0.99 (NO ₃ ⁻)	0.3
	3-C	5			5	1:1	0.99 (NO ₂ ⁻)	0.6
	3-D		5	5		1:1	0.99 (NO ₃ ⁻)	0.6
	3-E	5			5	1:1	0.99 (NO ₂ ⁻)	1.3
	3-F		5	5		1:1	0.99 (NO ₃ ⁻)	1.3
	3-G	5			5	1:1	0.99 (NO ₂ ⁻)	2.6
	3-H		5	5		1:1	0.99 (NO ₃ ⁻)	2.6
	3-I	5			5	1:1	0.99 (NO ₂ ⁻)	6.4
	3-J		5	5		1:1	0.99 (NO ₃ ⁻)	6.4
Control (November 2016)	4-A	5		0.4	10	0.54:1	0.93 (NO ₂ ⁻)	0
	4-B		5	5.4	5	0.54:1	0.50 (NO ₃ ⁻)	0
Oxygen manipulation (November 2016)	5-A	5		0.4	10	0.54:1	0.93 (NO ₂ ⁻)	0.2
	5-B		5	5.4	5	0.54:1	0.50 (NO ₃ ⁻)	0.2
	5-C	5		0.4	10	0.54:1	0.93 (NO ₂ ⁻)	0.4
	5-D		5	5.4	5	0.54:1	0.50 (NO ₃ ⁻)	0.4
	5-E	5		0.4	10	0.54:1	0.93 (NO ₂ ⁻)	1.9
	5-F		5	5.4	5	0.54:1	0.50 (NO ₃ ⁻)	1.9
	5-G	5		0.4	10	0.54:1	0.93 (NO ₂ ⁻)	4.2
	5-H		5	5.4	5	0.54:1	0.50 (NO ₃ ⁻)	4.2
	5-I	5		0.4	10	0.54:1	0.93 (NO ₂ ⁻)	7.3
	5-J		5	5.4	5	0.54:1	0.50 (NO ₃ ⁻)	7.3
Control (May 2017)	6-A	5		0.4	11.3	0.48:1	0.93 (NO ₂ ⁻)	0
	6-B		5	5.4	6.3	0.48:1	0.44 (NO ₃ ⁻)	0

363

364 **Table 1: Parameters for control, nitrogen manipulation and oxygen manipulation incubation experiments in July 2016, November**
365 **2016 and May 2017 sampling. In May 2017, only control experiment was conducted. The unit “μmol L⁻¹” is represented by “μM”.**
366 **Shaded columns highlight the concentrations for ¹⁵N tracers. In situ nitrate and nitrite concentrations in July 2016 were < 0.02**
367 **μmol L⁻¹; in November 2016 the concentrations were 5.0 and 0.4 μmol L⁻¹, respectively; in May 2017 the concentrations were 6.3**
368 **and 0.4 μmol L⁻¹, respectively.**

369

370

371

372 **5 Funding Sources and Acknowledgements**

373 This work is supported by the following funding sources: The PEI Grand Challenges – Control of Microbial Nitrous Oxide
374 Production in Coastal Waters to B.B.W.. National Science Foundation (OCE 1427019) to J.C.C.. German Academic Exchange
375 Service Postdoctoral Researchers International Mobility Experience fellowship to C.F. The authors would like to thank
376 Michael Owens at Horn Point Laboratory for his assistance with field research equipment. We thank Sergey Oleynik for
377 technical assistance during laboratory analysis.

378 **6 References**

- 379 Anderson, J. H.: The metabolism of hydroxylamine to nitrite by *Nitrosomonas*, *Biochem. J.*, 91, 8-17, 1964.
380
381 Arp, D. J., and Stein, L. Y.: Metabolism of inorganic N compounds by ammonia-oxidizing bacteria, *Crit Rev Biochem Mol Biol*, 38, 471-
382 495, doi:10.1080/10409230390267446, 2003.
383
384 Baird, D., Ulanowicz, R. E., and Boynton, W. R.: Seasonal Nitrogen Dynamics in Chesapeake Bay: a Network Approach, *Estuar. Coast.*
385 *Shelf Sci.*, 41, 137-162, doi:10.1006/ecss.1995.0058, 1995.
386
387 Beaulieu, J. J., Tank, J. L., Hamilton, S. K., Wollheim, W. M., Hall, R. O., Mulholland, P. J., Peterson, B. J., Ashkenas, L. R., Cooper, L.
388 W., Dahm, C. N., Dodds, W. K., Grimm, N. B., Johnson, S. L., McDowell, W. H., Poole, G. C., Valett, H. M., Arango, C. P., Bernot, M. J.,
389 Burgin, A. J., Crenshaw, C. L., Helton, A. M., Johnson, L. T., O'Brien, J. M., Potter, J. D., Sheibley, R. W., Sobota, D. J., and Thomas, S.
390 M.: Nitrous oxide emission from denitrification in stream and river networks, *Proc. Natl. Acad. Sci. U.S.A.*, 108, 214-219,
391 doi:10.1073/pnas.1011464108, 2011.
392
393 Boesch, D. F., Brinsfield, R. B., and Magnien, R. E.: Chesapeake Bay Eutrophication, *J. Environ. Qual.*, 30, 303-320,
394 doi:10.2134/jeq2001.302303x, 2001.
395
396 Bouskill, N. J., Eveillard, D., Chien, D., Jayakumar, A., and Ward, B. B.: Environmental factors determining ammonia-oxidizing organism
397 distribution and diversity in marine environments, *Environ. Microbiol.*, 14, 714-729, doi:10.1111/j.1462-2920.2011.02623.x, 2012.
398
399 Boynton, W. R., Garber, J. H., Summers, R., and Kemp, W. M.: Inputs, transformations, and transport of nitrogen and phosphorus in
400 Chesapeake Bay and selected tributaries, *Estuaries*, 18, 285-314, doi:10.2307/1352640, 1995.
401
402 Braman, R. S., and Hendrix, S. A.: Nanogram nitrite and nitrate determination in environmental and biological materials by vanadium(III)
403 reduction with chemiluminescence detection, *Anal. Chem.*, 61, 2715-2718, doi:10.1021/ac00199a007, 1989.
404
405 Bristow, L. A., Dalsgaard, T., Tiano, L., Mills, D. B., Bertagnolli, A. D., Wright, J. J., Hallam, S. J., Ulloa, O., Canfield, D. E., and Revsbech,
406 N. P.: Ammonium and nitrite oxidation at nanomolar oxygen concentrations in oxygen minimum zone waters, *Proc. Natl. Acad. Sci. U.S.A.*,
407 113, 10601-10606, doi:10.1073/pnas.1600359113, 2016.
408
409 Ciais, P., C. Sabine, G. Bala, L. Bopp, V. Brovkin, J. Canadell, A. Chhabra, R. DeFries, J. Galloway, M. Heimann, C. Jones, C. Le Quéré
410 R.B. Myneni, Piao, S., and Thornton, P.: Carbon and Other Biogeochemical Cycles, Cambridge, United Kingdom and New York, NY, USA,
411 465-570, 2013.
412
413 Cooper, S. R., and Brush, G. S.: A 2,500-Year History of Anoxia and Eutrophication in Chesapeake Bay, *Estuaries*, 16, 617-626,
414 doi:10.2307/1352799, 1993.
415

416 Dürr, H. H., Laruelle, G. G., van Kempen, C. M., Slomp, C. P., Meybeck, M., and Middelkoop, H.: Worldwide Typology of Nearshore
417 Coastal Systems: Defining the Estuarine Filter of River Inputs to the Oceans, *Estuaries Coasts*, 34, 441-458, doi:10.1007/s12237-011-9381-
418 y, 2011.

419

420 Eggleston, E. M., Lee, D. Y., Owens, M. S., Cornwell, J. C., Crump, B. C., and Hewson, I.: Key respiratory genes elucidate bacterial
421 community respiration in a seasonally anoxic estuary, *Environ. Microbiol.*, 17, 2306-2318, doi:10.1111/1462-2920.12690, 2015.

422

423 Elkins, J. W., Steven C. Wofsy, Michael B. McElroy, Charles E. Kolb, and Kaplan, W. A.: Aquatic sources and sinks for nitrous oxide,
424 *Nature*, 275, 602-606, doi:10.1038/275602a0, 1978.

425

426 Frame, C. H., and Casciotti, K. L.: Biogeochemical controls and isotopic signatures of nitrous oxide production by a marine ammonia-
427 oxidizing bacterium, *Biogeosciences*, 7, 2695-2709, doi:10.5194/bg-7-2695-2010, 2010.

428

429 Garcia, H. E., and Gordon, L. I.: Oxygen solubility in seawater: Better fitting equations, *Limnol. Oceanogr.*, 37, 1307-1312,
430 doi:10.4319/lo.1992.37.6.1307, 1992.

431

432 Garside, C.: A chemiluminescent technique for the determination of nanomolar concentrations of nitrate and nitrite in seawater, *Mar. Chem.*,
433 11, 159-167, doi:10.1016/0304-4203(82)90039-1, 1982.

434

435 Goreau, T. J., Kaplan, W. A., Wofsy, S. C., McElroy, M. B., Valois, F. W., and Watson, S. W.: Production of NO₂⁻ and N₂O by nitrifying
436 bacteria at reduced concentrations of oxygen, *Appl. Environ. Microbiol.*, 40, 526-532, 1980.

437

438 Graf, D. R. H., Jones, C. M., and Hallin, S.: Intergenomic Comparisons Highlight Modularity of the Denitrification Pathway and Underpin
439 the Importance of Community Structure for N₂O Emissions, *PLOS ONE*, 9, e114118, doi:10.1371/journal.pone.0114118, 2014.

440

441 Groffman, P. M., Williams, C. O., Pouyat, R. V., Band, L. E., and Yesilonis, I. D.: Nitrate leaching and nitrous oxide flux in urban forests
442 and grasslands, *J. Environ. Qual.*, 38, 1848-1860, doi:10.2134/jeq2008.0521, 2009.

443

444 Hagy, J. D., Boynton, W. R., Keefe, C. W., and Wood, K. V.: Hypoxia in Chesapeake Bay, 1950–2001: Long-term change in relation to
445 nutrient loading and river flow, *Estuaries*, 27, 634-658, doi:10.1007/BF02907650, 2004.

446

447 Hansen, H. P., and Koroleff, F.: Determination of nutrients, in: *Methods of Seawater Analysis*, Wiley-VCH Verlag GmbH, 159-228, 2007.

448

449 Hong, Y., Xu, X., Kan, J., and Chen, F.: Linking seasonal inorganic nitrogen shift to the dynamics of microbial communities in the
450 Chesapeake Bay, *Appl Microbiol Biotechnol*, 98, 3219, doi:10.1007/s00253-013-5337-4, 2014.

451

452 Horak, R. E. A., Qin, W., Schauer, A. J., Armbrust, E. V., Ingalls, A. E., Moffett, J. W., Stahl, D. A., and Devol, A. H.: Ammonia oxidation
453 kinetics and temperature sensitivity of a natural marine community dominated by Archaea, *ISME J*, 7, 2023-2033,
454 doi:10.1038/ismej.2013.75, 2013.

455

456 Jayakumar, A., O'Mullan, G. D., Naqvi, S. W. A., and Ward, B. B.: Denitrifying Bacterial Community Composition Changes Associated
457 with Stages of Denitrification in Oxygen Minimum Zones, *Microb. Ecol.*, 58, 350-362, doi:10.1007/s00248-009-9487-y, 2009.

458

459 Jayakumar, A., Peng, X., and Ward, B. B.: Community composition of bacteria involved in fixed nitrogen loss in the water column of two
460 major oxygen minimum zones in the ocean, *Aquatic Microbial Ecology*, 70, 245-259, doi:10.3354/ame01654, 2013.

461

462 Kana, T. M., Cornwell, J. C., and Zhong, L.: Determination of Denitrification in the Chesapeake Bay from Measurements of N₂^₂
463 Accumulation in Bottom Water, *Estuaries Coasts*, 29, 222-231, 2006.

464

465 Kaplan, W. A., Elkins, J. W., Kolb, C. E., McElroy, M. B., Wofsy, S. C., and Durán, A. P.: Nitrous oxide in fresh water systems: An estimate
466 for the yield of atmospheric N₂O associated with disposal of human waste, *Pure Appl. Geophys.*, 116, 423-438, doi:10.1007/bf01636897,
467 1978.

468

469 Kartal, B., Maalcke, W. J., de Almeida, N. M., Cirpus, I., Gloerich, J., Geerts, W., Op den Camp, H. J. M., Harhangi, H. R., Janssen-Megens,
470 E. M., Francoijs, K.-J., Stunnenberg, H. G., Keltjens, J. T., Jetten, M. S. M., and Strous, M.: Molecular mechanism of anaerobic ammonium
471 oxidation, *Nature*, 479, 127-130, doi:10.1038/nature10453, 2011.

472
473 Kemp, W., Sampou, P., Caffrey, J., Mayer, M., Henriksen, K., and Boynton, W. R.: Ammonium recycling versus denitrification in
474 Chesapeake Bay sediments, *Limnol. Oceanogr.*, 35, 1545-1563, 1990.
475
476 Kemp, W. M., Sampou, P. A., Garber, J., Tuttle, J., and Boynton, W. R.: Seasonal depletion of oxygen from bottom waters of Chesapeake
477 Bay: roles of benthic and planktonic respiration and physical exchange processes, *Mar. Ecol. Prog. Ser.*, 85, 137-152, 1992.
478
479 Larsen, R. K., Steinbacher, J. C., and Baker, J. E.: Ammonia exchange between the atmosphere and the surface waters at two locations in
480 the Chesapeake Bay, *Environ. Sci. Technol.*, 35, 4731-4738, doi:10.1021/es0107551, 2001.
481
482 Lee, D. Y., Owens, M. S., Crump, B. C., and Cornwell, J. C.: Elevated microbial CO₂ production and fixation in the oxic/anoxic interface
483 of estuarine water columns during seasonal anoxia, *Estuar. Coast. Shelf Sci.*, 164, 65-76, doi:10.1016/j.ecss.2015.07.015, 2015a.
484
485 Lee, D. Y., Owens, M. S., Doherty, M., Eggleston, E. M., Hewson, I., Crump, B. C., and Cornwell, J. C.: The Effects of Oxygen Transition
486 on Community Respiration and Potential Chemoautotrophic Production in a Seasonally Stratified Anoxic Estuary, *Estuaries Coasts*, 38, 104-
487 117, doi:10.1007/s12237-014-9803-8, 2015b.
488
489 Loughner, C. P., Tzortziou, M., Shroder, S., and Pickering, K. E.: Enhanced dry deposition of nitrogen pollution near coastlines: A case
490 study covering the Chesapeake Bay estuary and Atlantic Ocean coastline, *J. Geophys. Res.: Atmos.*, 121, 14,221-214,238,
491 doi:10.1002/2016JD025571, 2016.
492
493 McElroy, M. B., Elkins, J. W., Wofsy, S. C., Kolb, C. E., Durán, A. P., and Kaplan, W. A.: Production and release of N₂O from the Potomac
494 Estuary 1, *Limnol. Oceanogr.*, 23, 1168-1182, doi:10.4319/lo.1978.23.6.1168, 1978.
495
496 McIlvin, M. R., and Altabet, M. A.: Chemical conversion of nitrate and nitrite to nitrous oxide for nitrogen and oxygen isotopic analysis in
497 freshwater and seawater, *Anal. Chem.*, 77, 5589-5595, doi:10.1021/ac050528s, 2005.
498
499 Moir, J. W. B., and Wood, N. J.: Nitrate and nitrite transport in bacteria, *Cell. Mol. Life Sci.*, 58, 215-224, doi:10.1007/PL00000849, 2001.
500
501 Peng, X., Fuchsman, C. A., Jayakumar, A., Warner, M. J., Devol, A. H., and Ward, B. B.: Revisiting nitrification in the Eastern Tropical
502 South Pacific: A focus on controls, *J. Geophys. Res.: Oceans*, 121, 1667-1684, doi:10.1002/2015JC011455, 2016.
503
504 Poth, M., and Focht, D. D.: (15)N Kinetic Analysis of N(2)O Production by *Nitrosomonas europaea*: an Examination of Nitrifier
505 Denitrification, *Appl. Environ. Microbiol.*, 49, 1134-1141, 1985.
506
507 Nitrogen Loads to the Chesapeake Bay by Source: <http://www.chesapeakeprogress.com/clean-water/watershed-implementation-plans>,
508 access: August 28, 2017.
509
510 Qin, W., Meinhardt, K. A., Moffett, J. W., Devol, A. H., Virginia Armbrust, E., Ingalls, A. E., and Stahl, D. A.: Influence of oxygen
511 availability on the activities of ammonia-oxidizing archaea, *Environ. Microbiol. Rep.*, 9, 250-256, doi:10.1111/1758-2229.12525, 2017.
512
513 Ravishankara, A., Daniel, J. S., and Portmann, R. W.: Nitrous oxide (N₂O): the dominant ozone-depleting substance emitted in the 21st
514 century, *Science*, 326, 123-125, 2009.
515
516 Rich, J. J., Dale, O. R., Song, B., and Ward, B. B.: Anaerobic ammonium oxidation (anammox) in Chesapeake Bay sediments, *Microb.*
517 *Ecol.*, 55, 311-320, doi:10.1007/s00248-007-9277-3, 2008.
518
519 Russell, K. M., Galloway, J. N., Macko, S. A., Moody, J. L., and Scudlark, J. R.: Sources of nitrogen in wet deposition to the Chesapeake
520 Bay region, *Atmos. Environ.*, 32, 2453-2465, doi:10.1016/S1352-2310(98)00044-2, 1998.
521
522 Santoro, A. E., Buchwald, C., McIlvin, M. R., and Casciotti, K. L.: Isotopic Signature of N₂O Produced by Marine Ammonia-Oxidizing
523 Archaea, *Science*, 333, 1282-1285, doi:10.1126/science.1208239, 2011.
524
525 Schilt, A., Baumgartner, M., Blunier, T., Schwander, J., Spahni, R., Fischer, H., and Stocker, T. F.: Glacial–interglacial and millennial-scale
526 variations in the atmospheric nitrous oxide concentration during the last 800,000 years, *Quat. Sci. Rev.*, 29, 182-192,
527 doi:10.1016/j.quascirev.2009.03.011, 2010.

528 Seitzinger, S. P., and Kroeze, C.: Global distribution of nitrous oxide production and N inputs in freshwater and coastal marine ecosystems,
529 *Glob. Biogeochem. Cycles*, 12, 93-113, doi:10.1029/97GB03657, 1998.

530

531 Taft, J. L., Taylor, W. R., Hartwig, E. O., and Loftus, R.: Seasonal oxygen depletion in Chesapeake Bay, *Estuaries*, 3, 242-247,
532 doi:10.2307/1352079, 1980.

533

534 Thompson, R. L., Chevallier, F., Crotwell, A. M., Dutton, G., Langenfelds, R. L., Prinn, R. G., Weiss, R. F., Tohjima, Y., Nakazawa, T.,
535 Krummel, P. B., Steele, L. P., Fraser, P., O'Doherty, S., Ishijima, K., and Aoki, S.: Nitrous oxide emissions 1999 to 2009 from a global
536 atmospheric inversion, *Atmos. Chem. Phys.*, 14, 1801-1817, doi:10.5194/acp-14-1801-2014, 2014.

537

538 Weigand, M. A., Foriel, J., Barnett, B., Oleynik, S., and Sigman, D. M.: Updates to instrumentation and protocols for isotopic analysis of
539 nitrate by the denitrifier method, *Rapid Commun. Mass Spectrom.*, 30, 1365-1383, doi:10.1002/rcm.7570, 2016.

540

541 Weiss, R. F., and Price, B. A.: Nitrous oxide solubility in water and seawater, *Mar. Chem.*, 8, 347-359, doi:10.1016/0304-4203(80)90024-
542 9, 1980.

543

544 Wilson, S. T., del Valle, D. A., Segura-Noguera, M., and Karl, D. M.: A role for nitrite in the production of nitrous oxide in the lower
545 euphotic zone of the oligotrophic North Pacific Ocean, *Deep-Sea Res. I*, 85, 47-55, doi:10.1016/j.dsr.2013.11.008, 2014.

546

547 Zhou, Y., Scavia, D., and Michalak, A. M.: Nutrient loading and meteorological conditions explain interannual variability of hypoxia in
548 Chesapeake Bay, *Limnol. Oceanogr.*, 59, 373-384, doi:10.4319/lo.2014.59.2.0373, 2014.

549

550 Zhu, X., Burger, M., Doane, T. A., and Horwath, W. R.: Ammonia oxidation pathways and nitrifier denitrification are significant sources of
551 N₂O and NO under low oxygen availability, *Proc. Natl. Acad. Sci. U.S.A.*, 110, 6328-6333, doi:10.1073/pnas.1219993110, 2013.

552

553

554